A Self-Calibration Concept for Establishing the Complex Measurement Ability of Homodyne Network Analyzers

HERMANN-JOSEF EUL, STUDENT MEMBER, IEEE, AND BURKHARD SCHIEK, MEMBER, IEEE

Abstract—**A homodyne phase shifter controlled double reflectometer is presented. Its ability to make complex measurements of a network depends on a knowledge of the phase shifter characteristics. This knowledge is established using fully unknown standards merely by exploiting reciprocity. If a system error correction is performed, the data needed for error correction contain enough information to determine the behavior of the phase shifter and no additional standards are needed. It is shown by simulation that the measurement of the parameters of the device under test is only weakly influenced by errors in the phase shifter behavior.**

I. Introduction

NETWORK analyzers today are in widespread use. Mostly they are based on the well-known heterodyne concept; that is, the RF signal is down-converted to an IF signal to measure the complex information, namely magnitude and phase. Another way to make microwave measurements automatically is by the six-port network analyzer [3], which uses power detectors. A third way has also been proposed, the homodyne network analyzer [1], which uses a coherent detection via mixers. In contrast to power detectors, coherent detection with mixers is a linear detection, providing a higher dynamic range. Unfortunately the output signal is proportional not to the complex but to the real part of the RF information; therefore a further measurement is necessary to obtain information about the imaginary part, requiring a 90° phase shifter. Phase shifts φ different from 90° are possible, but they must be known exactly. Although the homodyne concept is very simple and uses an inexpensive RF part, the lack of phase shifters with a known phase shift is one reason that homodyne concepts are not in use for commercially available laboratory measurement equipment. Therefore the possibility of determining the effective phase shift of the imperfect device *in situ* has been investigated. With the procedure described below, the homodyne detector is indeed able to measure complex information of the RF signal, thereby establishing a complex measurement capability. Once the complex measurement capability is established, the setup can be calibrated in the same way as a heterodyne network analyzer to remove system errors. However, due to measurement errors, e.g. noise or quantization, the complex measurement ability cannot be established without error. These errors lead to small errors in the determination of the calibration constants and they ultimately influence the accuracy of the measurement of the device under test (DUT).

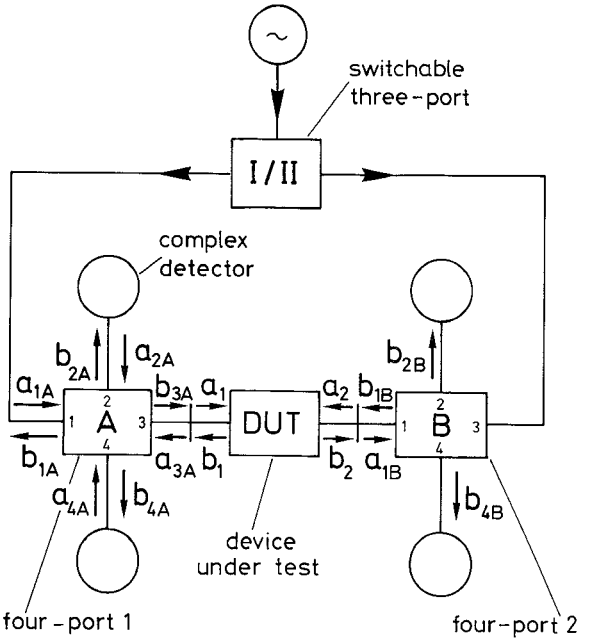

Fig. 1. The principal block diagram of the setup.

II. Theory

A. General Description

For the mathematical description in this section a setup is examined which is capable of making four complex measurements (see Fig. 1). First we treat four-port 1, depicted at the left side. It is introduced to provide a measure of the wave propagating toward the device under test as well as a measure of the wave emerging from the DUT; e.g., b_{4A} is proportional to the incident wave and b_{2A} to the reflected wave. Due to such imperfections as a finite directivity or mismatched ports, both measurements are disturbed. Thus in our discussion any four-port is

Manuscript received March 21, 1989; revised October 19, 1989. This work was supported by the Deutsche Forschungsgemeinschaft (DFG).

The authors are with the Institut für Hoch-und Höchstfrequenztechnik, Ruhr-Universität Bochum, P.O. Box 10 21 48, 4630 Bochum 1, West Germany.

IEEE Log Number 8933244.

0018-9480/90/0300-0284$01.00 ©1990 IEEE

allowed so long as the readings of b_{2A} and b_{4A} are independent of each other.

Without loss of generality we introduce a fictitious four-port A which includes the four-port 1 and the mismatches and losses of the detectors connected. Therefore $a_{2A} = a_{4A} = 0$ and

$$b_{1A} = S_{11A}a_{1A} + S_{13A}a_{3A} \quad (1)$$

$$b_{2A} = S_{21A}a_{1A} + S_{23A}a_{3A} \quad (2)$$

$$b_{3A} = S_{31A}a_{1A} + S_{33A}a_{3A} \quad (3)$$

$$b_{4A} = S_{41A}a_{1A} + S_{43A}a_{3A}. \quad (4)$$

These four equations can be reduced in a straightforward way to the relationship

$$\begin{pmatrix} b_{2A} \\ b_{4A} \end{pmatrix} = \begin{pmatrix} A_{11} & A_{12} \\ A_{21} & A_{22} \end{pmatrix} \begin{pmatrix} a_{3A} \\ b_{3A} \end{pmatrix}. \quad (5)$$

In a similar manner, four-port 2 is treated, yielding

$$\begin{pmatrix} b_{2B} \\ b_{4B} \end{pmatrix} = \begin{pmatrix} B_{11} & B_{12} \\ B_{21} & B_{22} \end{pmatrix} \begin{pmatrix} b_{1B} \\ a_{1B} \end{pmatrix}. \quad (6)$$

For any two-port, i.e., a DUT or a calibration standard, connected to the measurement ports

$$\begin{pmatrix} b_1 \\ a_1 \end{pmatrix} = \begin{pmatrix} T_{11} & T_{12} \\ T_{21} & T_{22} \end{pmatrix} \begin{pmatrix} a_2 \\ b_2 \end{pmatrix} \quad (7)$$

holds, where the T_{ij} are the elements of the wave transmission matrix [7]. Using the boundary conditions

$$b_1 = a_{3A} \quad a_1 = b_{3A} \quad a_2 = b_{1B} \quad \text{and} \quad b_2 = a_{1B} \quad (8)$$

the equation

$$\begin{pmatrix} b_{2A} \\ b_{4A} \end{pmatrix} = \begin{pmatrix} A_{11} & A_{12} \\ A_{21} & A_{22} \end{pmatrix} \begin{pmatrix} T_{11} & T_{12} \\ T_{21} & T_{22} \end{pmatrix} \begin{pmatrix} B_{11} & B_{12} \\ B_{21} & B_{22} \end{pmatrix}^{-1} \begin{pmatrix} b_{2B} \\ b_{4B} \end{pmatrix}$$

$$= \boldsymbol{ATB}^{-1} \begin{pmatrix} b_{2B} \\ b_{4B} \end{pmatrix} \quad (9)$$

is derived. In order to provide a second vector equation of this type, the three-port (Fig. 1) is turned to its second position, position II. This might be the second position of a microwave switch, but any alteration of its signal-splitting behavior is sufficient. However, a microwave switch may be a preferred realization. The readings in the second state of the three-port are indicated by the prime and fit

$$\begin{pmatrix} b'_{2A} \\ b'_{4A} \end{pmatrix} = \boldsymbol{ATB}^{-1} \begin{pmatrix} b'_{2B} \\ b'_{4B} \end{pmatrix}. \quad (10)$$

These two vector equations (eqs. (9) and (10)) are combined to the matrix equation

$$\begin{pmatrix} b_{2A} & b'_{2A} \\ b_{4A} & b'_{4A} \end{pmatrix} = \boldsymbol{ATB}^{-1} \begin{pmatrix} b_{2B} & b'_{2B} \\ b_{4B} & b'_{4B} \end{pmatrix} \quad (11)$$

which is finally denoted as

$$\boldsymbol{ATB}^{-1} = \begin{pmatrix} b_{2A} & b'_{2A} \\ b_{4A} & b'_{4A} \end{pmatrix} \begin{pmatrix} b_{2B} & b'_{2B} \\ b_{4B} & b'_{4B} \end{pmatrix}^{-1} \stackrel{\text{def}}{=} \boldsymbol{M}. \quad (12)$$

This description is usually the starting point of network analyzer calibration theory based on complex measuring heterodyne detection. The matrices $\boldsymbol{A}$ and $\boldsymbol{B}^{-1}$ are the well-known error matrices considering the imperfections of the setup.

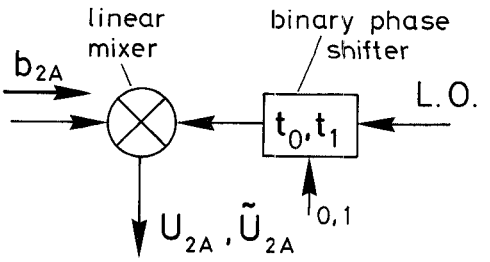

Fig. 2. A homodyne detector with an effective binary phase shift $t_{0,1} = |t_{0,1}|e^{j\varphi_{0,}}$.

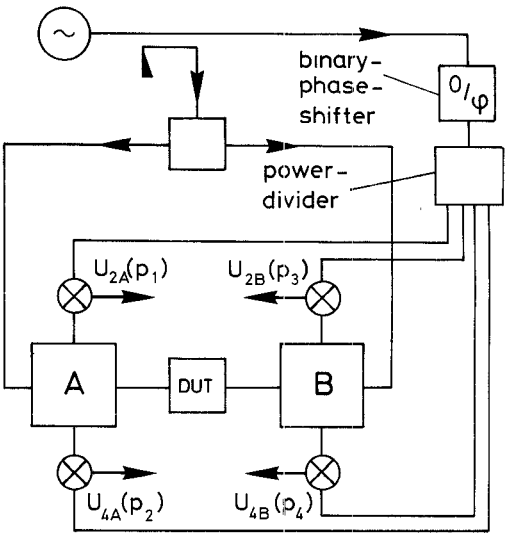

Fig. 3. The homodyne double reflectometer.

If it is possible to provide the measurement matrix $\boldsymbol{M}$ also with a homodyne setup, one is able to proceed with any calibration procedure relying on a formalism similar to (12). This might be, for example, the TSD procedure [2], the TRL procedure [3], the TMR, or the TAN procedure [4].

B. Establishing a Complex Measurement Ability

In this subsection the complex measurement ability is established without an additional expense of calibration standards. This means that either no further standard or only fully unknown standards are required.

Therefore the behavior of one of the coherent detectors will be examined further (Fig. 2), e.g. the detection of b_{A2}. If the phase shifter in the path of the local oscillator is switched off, the detected voltage will be denoted U_{2A} and if it is turned on, the same quantity will be $\tilde{U}_{2A}$. It can easily be seen that these two voltages can be assembled to reconstruct the complex wave b_{2A} by

$$b_{2A} = \alpha_{2A}(U_{2A} + p\tilde{U}_{2A}), \stackrel{\text{def}}{=} \alpha_{2A}U_{2A}(p) \quad (13)$$

where α_{2A} is a complex proportionality factor. At this time the "weighting factor" p is still unknown. For example, if

the phase shifter is an ideal one, i.e., a minus 90° phase shifter, p equals j and therefore $U_{2A}(p) = U_{2A} + j\tilde{U}_{2A}$.

If the phase shifter is in the common path of the mixers (see Fig. 3), the factor p is the same for all mixers. This assumption is not strictly valid. But if the phase shifter only shows a small parasitic amplitude modulation and if the mixers are fairly equal, the error is of a higher order small. Nevertheless, more general solutions are also available in which each detector may have another weighting factor, denoted by the weighting vector $\underline{p} = (p_1, p_2, p_3, p_4)$. However, $\underline{p}$ has to be determined by some kind of calibration procedure. Therefore (13) and similar equations for the other complex waves will be substituted into (11), leading to

$$\begin{pmatrix} U_{2A}(p_1) & U'_{2A}(p_1) \\ U_{4A}(p_2) & U'_{4A}(p_2) \end{pmatrix} = \boldsymbol{ATB}^{-1} \begin{pmatrix} U_{2B}(p_3) & U'_{2B}(p_3) \\ U_{4B}(p_4) & U'_{4B}(p_4) \end{pmatrix} \tag{14}$$

$$\rightarrow \boldsymbol{M}_A(\underline{p}) = \boldsymbol{ATB}^{-1}\boldsymbol{M}_B(\underline{p})$$

$$\rightarrow \boldsymbol{ATB}^{-1} = \boldsymbol{M}_A(\underline{p})\boldsymbol{M}_B(\underline{p})^{-1} = \boldsymbol{M}(\underline{p}) \tag{15}$$

in which the proportionality factors α_i are included in the error matrices $\boldsymbol{A}$ and $\boldsymbol{B}^{-1}$.

In order to determine the weighting vector $\underline{p}$ a number of completely unknown calibration two-ports with the wave transmission matrices $\boldsymbol{N1}$ and $\boldsymbol{N2}$ are connected to the measurement ports, leading to the measurement matrices which are functions of p:

$$\boldsymbol{M1}(\underline{p}) = \boldsymbol{AN1B}^{-1} \tag{16}$$

$$\boldsymbol{M2}(\underline{p}) = \boldsymbol{AN2B}^{-1}, \cdots. \tag{17}$$

Taking the inverse of $\boldsymbol{M1}(\underline{p})$ and multiplying by $\boldsymbol{M2}(\underline{p})$, the new matrix is denoted as

$$\boldsymbol{Q}(p) = \boldsymbol{M2}(\underline{p})\boldsymbol{M1}(\underline{p})^{-1}$$

$$= \left(\boldsymbol{M2}_A(\underline{p})\boldsymbol{M2}_B(\underline{p})^{-1}\right)\left(\boldsymbol{M1}_A(\underline{p})\boldsymbol{M1}_B(\underline{p})^{-1}\right)^{-1} \tag{18}$$

with the determinant

$$\det \boldsymbol{Q}(\underline{p}) = \frac{\det \boldsymbol{M2}_A(\underline{p}) \det \boldsymbol{M1}_B(\underline{p})}{\det \boldsymbol{M2}_B(\underline{p}) \det \boldsymbol{M1}_A(\underline{p})}. \tag{19}$$

On the other hand it is also true that

$$\det \boldsymbol{Q}(\underline{p}) = \det(\boldsymbol{M2M1}^{-1})$$

$$= \det\left(\boldsymbol{AN2B}^{-1}(\boldsymbol{AN1B}^{-1})^{-1}\right) = \frac{\det \boldsymbol{N2}}{\det \boldsymbol{N1}}. \tag{20}$$

If $\boldsymbol{N1}$ and $\boldsymbol{N2}$ are the transmission matrices of reciprocal but otherwise unknown two-ports, their determinants equal 1:

$$\det \boldsymbol{N1} = \det \boldsymbol{N2} = 1 \tag{21}$$

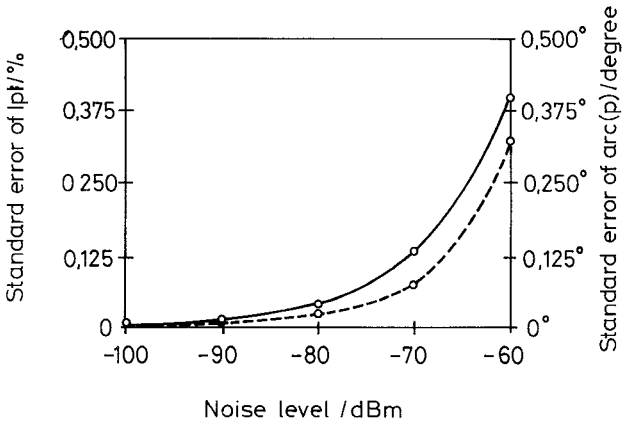

Fig. 4. Standard error of the weighting factor p versus noise level P_n.
—— Standard error $\sigma(|p|)$ of the magnitude.
---- Standard error $\sigma(\arg(p))$ of the argument.

and therefore

$$\det \boldsymbol{M2}_A(\underline{p}) \det \boldsymbol{M1}_B(\underline{p}) - \det \boldsymbol{M2}_B(\underline{p}) \det \boldsymbol{M1}_A(\underline{p}) \stackrel{!}{=} 0 \tag{22}$$

holds.

The number of necessary characteristic equations similar to (22), and therefore the number of unknown reciprocal two-ports, depend on the number of different elements in the weighting vector $\underline{p}$.

In the case described above for which $p_1 = p_2 = p_3 = p_4 = p$ holds, two unknown standards are needed. Then a further algebraic treatment leads to a polynomial characteristic equation of the fourth degree:

$$a_4 p^4 + a_3 p^3 + a_2 p^2 + a_1 p + a_0 = 0 \tag{23}$$

which must be satisfied by the weighting factor p and can be solved by various methods. Good results have been obtained using Müller's method [5]. As has been discussed in [6], eq. (23) always has one unique solution. However, a linear solution is also possible, for example, to provide starting values for the nonlinear solution. This linear solution can be applied at the expense of one more unknown standard [6].

In the most general case of four different weighting factors, four unknown standards are necessary to provide the four characteristic equations needed:

$$\sum_{n=0}^{1}\sum_{m=0}^{1}\sum_{k=0}^{1}\sum_{l=0}^{1} a_{i,l+2k+4m+8n} p_4^n p_3^m p_2^k p_1^l = 0, \quad i = 1,2,3,4. \tag{24}$$

These can be solved numerically as well.

III. Discussion

A. Accuracy of the Weighting Factors

If the input data are not exact the performance drops with increasing measurement errors. Therefore attention is given to the way in which the calculated weighting vector differs from the ideal one if the input data become noisy. The simulations are performed under practical assumptions regarding losses ($\approx 0.1 \cdots 0.5$ dB for each component), mismatches ($\approx -15 \cdots -20$ dB), finite directivities

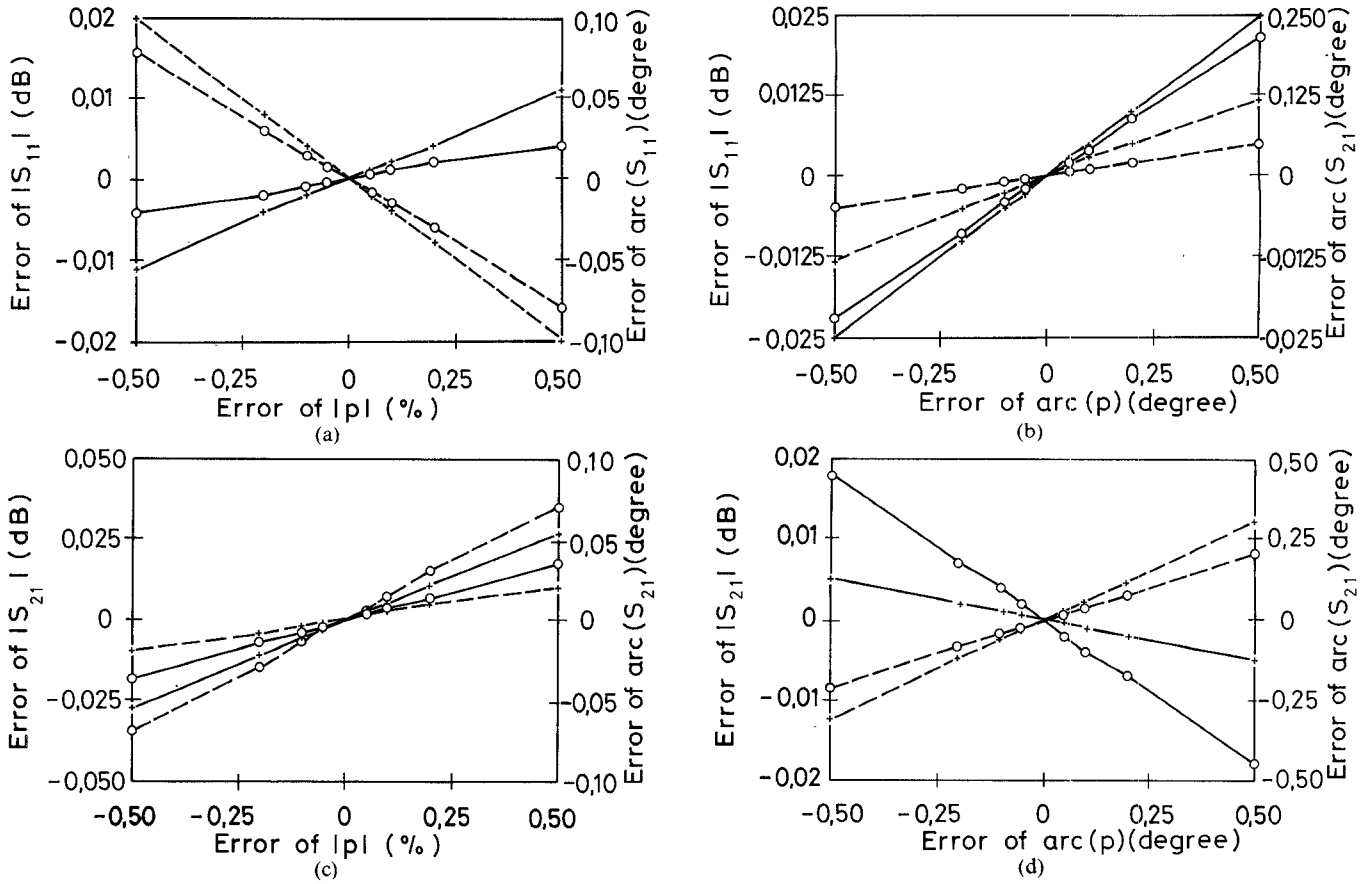

Fig. 5. Errors of the parameters of the DUT's (55 Ω and 100 Ω transmission lines) versus the error in the weighting vector:

——— Error of the magnitude, i.e., $20\log(|\hat{S}_{ij}|) - 20\log(|S_{ij}|)$.

---- Error of the argument, i.e., $\arg(\hat{S}_{ij}) - \arg(S_{ij})$.

S_{ij}: Exact values:
+: $|S_{11}| = -20.45$ dB, $\arg(S_{11}) = 0°$;
$|S_{21}| = -0.04$ dB, $\arg(S_{21}) = 90°$;
○: $|S_{11}| = -4.44$ dB, $\arg(S_{11}) = 0°$;
$|S_{21}| = -1.94$ dB, $\arg(S_{21}) = 90°$.

$\hat{S}_{ij}$: Evaluated values using nonideal weighting factors.

(≈ -15 dB), switching-dependent mismatches (≈ -15 dB), crosstalk ($\approx -20 \cdots -40$ dB), etc. The weighting factors are assumed to be $p_i = j = e^{j90°}$, $i = 1,2,3,4$. The source provides 3 dBm of microwave power and the noise level in the measurement channels is assumed to be variable.

In Fig. 4 the standard error of the weighting factor is plotted as a function of the noise level.

However, the simulations show that the standard error of the weighting factor magnitude remains for practical noise levels (less than -80 dBm) better than 0.04 percent, which is well below any measurement accuracy. As to be expected from a random phasor model, the corresponding standard error of the argument is $0.02° \approx \arcsin(0.04 \text{ percent}/100 \text{ percent})$. This means that measurement errors due to thermal noise or quantization noise are not influencing the accuracy of the weighting factor noticeably.

B. Accuracy of Measurements

In this subsection the way in which the measurement performance of the setup drops if the weighting factors are not exactly evaluated is investigated. The reason for the reduced measurement performance is that the reconstructed complex waves will show some errors due to an imperfect weighting factor. Actually they become a linear superposition of the original wave and its complex conjugate, e.g.,

$$U_{2A}(p_1) = b_{2A} + \beta_{2A} b_{2A}^{*}. \tag{25}$$

In (25) the factor β_{2A} becomes zero if the weighting factor p_1 has been determined exactly and is equivalent to the image rejection factor of a single-sideband receiver.

In order to show the impact of these errors on the final measurements, simulations have been undertaken relying on the same conditions as mentioned above. The "measured" data have been corrected from system errors using the TAN procedure [4]. The DUT's were assumed to be transmission lines with an electrical length of 90° and characteristic impedances of 55 Ω and 100 Ω, respectively. Fig. 5(a) shows the deviation of the measured value of S_{11} from the ideal measurement versus the error in amplitude of the weighting factors. In Fig. 5(b) the same quantity is plotted versus the error in the argument of the weighting

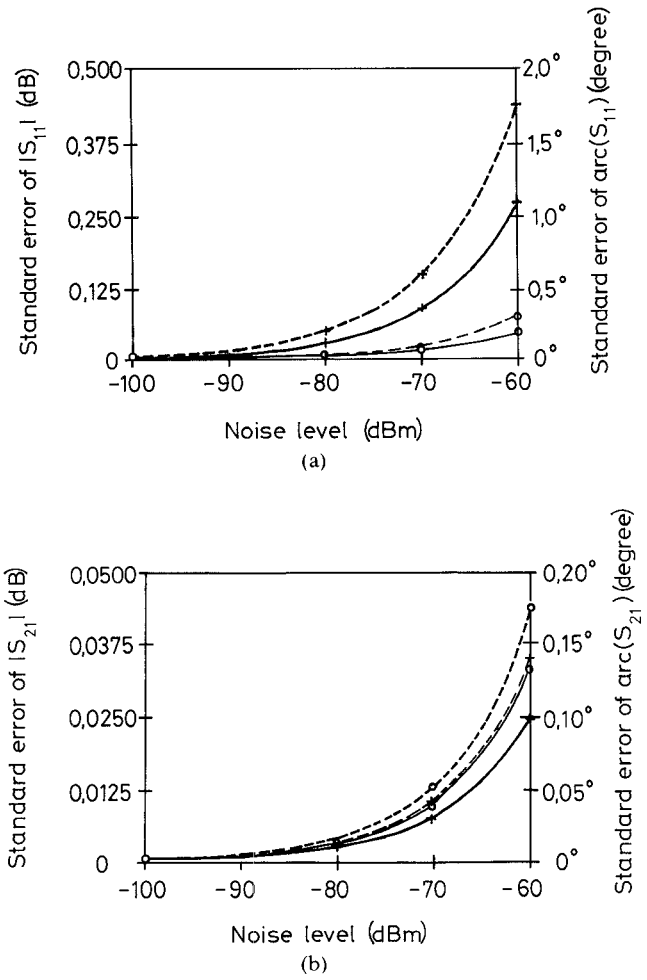

Fig. 6. Standard errors of the parameters of the DUT (55 Ω and 100 Ω transmission lines) versus noise level P_n:

——— Standard error of the magnitude, i.e., $20\log(|S_{ij}|+\sigma(|\hat{S}_{ij}|))-20\log(|S_{ij}|)$.

– – – – Standard error of the argument, i.e., $\sigma(\arg(\hat{S}_{ij}))$.

S_{ij}: Exact values (see Fig. 5).

$\hat{S}_{ij}$: Evaluated values using noisy data for system error calibration and DUT measurement. System error removal has been performed by using the TAN procedure.

factors. Fig. 5(c) and Fig. 5(d) show similar results for the transmission coefficient S_{21}.

The deviations from the correct values given by Fig. 5 are caused only by imperfect weighting factors. They should be compared to those which arise from noisy measurement data and which occur in homodyne as well as heterodyne systems. In Fig. 6 the way in which S_{11} and S_{21} are degraded is plotted versus noise level in the detection channels for a perfect complex measurement ability. Notice that this is not the signal-to-noise ratio but the total power of noise in each detection channel and 3 dBm total power fed into the switchable three-port (Figs. 1 and 3). Although in practice the noise level may be well below the values used in Fig. 6, they make it possible to compare the direct impact of the noise level on the measurement with the indirect influence via the weighting factors.

However, the loci show that normal measurement errors due to noise are of the same order as the errors caused by imperfectly evaluated weighting factors due to noisy data. This means that errors in the weighting vector proved to be noncritical as they do not lead to enhanced errors in the final results.

In order to obtain the predicted behavior in a practical setup, one has to pay attention to certain details. For example there must be no crosstalk between the measurement channels via the LO network. This is normally ensured by the RF-to-LO isolation of the mixers and the decoupling of the power divider in the LO feeding network. If this is not sufficient, isolators must be inserted into the LO feeding paths. However, crosstalk between the measurement channels for almost any arbitrary path in the test section of the RF part of the setup is allowed and completely covered by the theory. However, the model does not cover leakage between the two reflectometers. In a similar practical homodyne setup where the above-mentioned provisions among others have been applied, a dynamic range for the transmission coefficient of better than 100 dB has been achieved [8], [9].

IV. Conclusion

Via the measurement of two *arbitrary* and *unknown* but *reciprocal* networks, it is possible to determine the complex weighting factor p, i.e., to establish the ability of measuring complex information in a homodyne network analyzer. As one example this can be done by using a sliding line of arbitrary characteristic impedance and unknown length and arbitrary reflections.

In order to reduce the effort of connecting calibration standards, it is possible to use the data needed anyway to calibrate the setup for system error removal. Calibration procedures such as TSD [2], TRL [3], TAN, and TMR [4] provide well-conditioned characteristic equations. Therefore it is possible to establish the ability of complex measurements without any additional expense and to proceed as in a normal network analyzer calibration.

References

[1] R. J. King, *Microwave Homodyne Systems*. London: Peter Peregrinus, 1978.

[2] N. R. Franzen and R. A. Speciale, "A new procedure for system calibration and error removal in automated *S*-parameter measurements," in *Proc. 5th European Microwave Conf.* (Hamburg), 1975, pp. 69–73.

[3] G. F. Engen and C. A. Hoer, "Thru-reflect-line: An improved technique for calibrating the dual six port automatic network analyzer," *IEEE Trans. Microwave Theory Tech.*, vol. MTT-27, pp. 987–993, Dec. 1979.

[4] H. J. Eul and B. Schiek, "Thru-match-reflect: One result of a rigorous theory for de-embedding and network analyzer calibration," in *Proc. 18th European Microwave Conf.* (Stockholm), 1988, pp. 909–914.

[5] H. R. Schwarz, *Numerische Mathematik* Stuttgart: Teubner Verlag, 1986.

[6] H. J. Eul, "Establishing the complex measurement ability of a homodyne network analyzer via self-calibration," in *1989 IEEE MTT-S Int. Microwave Symp. Dig.* (Long Beach), pp. 1187–1190

[7] P. I. Somlo and J. D. Hunter, *Microwave Impedance Measurements*. London: Peter Peregrinus, 1985.

[8] J. Schneider, U. Gärtner, and B. Schiek, "Crosstalk suppression for modulated subcarrier measurement systems," in *Proc. 17th European Microwave Conf.* (Rome), 1987, pp. 287–292.

[9] U. Gärtner, J. Schneider, and B. Schiek, "Homodyne network analysis—Improving the accuracy and sensitivity by redundant phase coding and double modulation," *Arch. Elek. Übertragung.*, vol. 43, no. 1, pp. 16–22, 1989.

✠

Hermann-Josef Eul (S'88) was born in Neustadt/Wied, Federal Republic of Germany, in 1959. He received the Dipl.-Ing. (FH) degree from the Fachhochschule Koblenz in 1984 and the Dipl.-Ing. degree from the University of Bochum in 1987, both in electrical engineering. He is currently working as a research assistant at the University of Bochum and is concerned with microwave measurement techniques.

Burkhard Schiek (M'85) was born in Elbing, Germany, on October 14, 1938. He received the Dipl.-Ing. and the Dr.-Ing. degrees in electrical engineering, both from the Technische Universität Braunschweig, Germany, in 1964 and 1966, respectively.

From 1964 to 1969, he was an Assistant at the Institut für Hochfrequenztechnik of the Technische Universität Braunschweig, where he worked on frequency multipliers, parametric amplifiers, and varactor phase shifters. From 1966 to 1969, he was involved in MIS interface physics and in the development of MIS varactors. From 1969 to 1978, he was with the Microwave Application Group of the Philips Forschungslaboratorium Hamburg GmbH, Hamburg, Germany, where he was mainly concerned with the stabilization of solid-state oscillators, oscillator noise, microwave integration, and microwave systems. Since 1978, he has been a Professor in the Department of Electrical Engineering, Ruhr-Universität Bochum, Germany, working on high-frequency measurement techniques and industrial applications of microwaves.